LA-UR-01-0088
Approved for public release; distribution is unlimited.

Title: **In-vivo diagnosis of chemically induced melanoma in an animal model using UV-visible and NIR elastic-scattering spectroscopy: preliminary testing**

Author(s): Ousama M. A'Amar, Ronald D. Ley, Paul M. Ripley, Irving J. Bigio

Submitted to:

In-vivo diagnosis of chemically induced melanoma in an animal model using UV-visible and NIR elastic-scattering spectroscopy: preliminary testing

Ousama M. A'Amar[1], Ronald D. Ley[2], Paul M. Ripley[1], Irving J. Bigio[1]

1 Bioscience Division, BS-1, MS: E535, Los Alamos National Laboratory, Los Alamos, NM 87544
2 University of New Mexico school of Medicine, Albuquerque, NM 87131

ABSTRACT

Elastic light scattering spectroscopy (ESS) has the potential to provide spectra that contain both morphological and chromophore information from tissue. We report on a preliminary study of this technique, with the hope of developing a method for diagnosis of highly-pigmented skin lesions, commonly associated with skin cancer. Four opossums were treated with dimethylbenz(a)anthracene to induce both malignant melanoma and benign pigmented lesions. Skin lesions were examined *in vivo* using both UV-visible and near infrared (NIR) ESS, with wavelength ranges of 330-900 nm and 900-1700 nm, respectively. Both portable systems used identical fiber-optic probe geometry throughout all of the measurements. The core diameters for illuminating and collecting fibers were 400 and 200 μm, respectively, with center-to-center separation of 350 μm. The probe was placed in optical contact with the tissue under investigation. Biopsies from lesions were analyzed by two standard histopathological procedures. Taking into account only the biopsied lesions, UV-visible ESS showed distinct spectral correlation for 11/13 lesions. The NIR-ESS correlated well with 12/13 lesions correctly.
The results of these experiments showed that UV-visible and NIR-ESS have the potential to classify benign and malignant skin lesions, with encouraging agreement to that provided by standard histopathological examination. These initial results show potential for ESS based diagnosis of pigmented skin lesions, but further trials are required in order to substantiate the technique.

Keywords: Cancer diagnosis, Fiber-optic probe, Elastic-scattering Spectroscopy, Melanoma, Optical Biopsy.

1. INTRODUCTION

Recent advances in several areas of optical technology have led to the development of several "optical biopsy" techniques. These methods offer a range of modalities for diagnosis, and include elastic-scattering spectroscopy (ESS), light-induced fluorescence spectroscopy (LIFS), optical coherence tomography (OCT), and Raman and vibrational spectroscopy. ESS, sometimes called diffuse-reflectance spectroscopy, is a particularly attractive technique since it provides spectra that contain information about the morphology of the tissue as well as the chromophore content (e.g. hemoglobin and melanin). Also, because ESS translates tissue morphological changes into spectral features, it can be compared with to the standard histopathologic examination, which is commonly based on the analysis of tissue structure (1,2). Furthermore, ESS has the potential for detecting the architectural changes at the cellular and sub-cellular level (6), which accompany both changes in tissue pathology and also different tissue types (2). Hence, ESS may be an appropriate technique for cancer diagnosis, with the advantage of avoiding tissue removal and providing diagnostic signatures *in situ,* noninvasively and in real time.
It therefore seemed appropriate to employ the Los Alamos optical ESS, to determine whether the technique could detect differences in pigmented skin lesions. ESS is sensitive to changes in light scattering, which is known to be dominant in skin, as well as detecting the presence of major absorbers such as water, blood, keratin and melanin. Cutaneous melanomas normally manifest themselves as a brown/black pigmented area on the surface of the skin, which is sometimes raised. In their early stage they may be confused with benign pigmented skin areas, e.g. benign nevi (8). As a preliminary test of the potential of ESS for diagnosing pigmented skin lesions, four opossums were treated with dimethylbenz(a)anthracene to induce malignant melanoma and benign pigmented lesions. Twenty-six lesions were examined *in vivo* using both UV-visible and near infrared (NIR) ESS. However, since only 13 of the lesions were biobsied and subjected to histopathological assisment, we report on only those results. The logic for testing the NIR system was to reduce the effects of melanin absorption, which dominates in the UV-visible region but is much weaker in the NIR

2. MATERIALS AND METHODS

2.1 Animals

Animals were from the breeding colony maintained at the Southwest Foundation for Biomedical Research (San Antonio, TX). The University of New Mexico Institutional Animal Care and Use Committee approved protocols were used in this study.

2.2. Treatment with 7, 12-dimethylbenz(a)anthracene (DMBA)

Prior to treatment, animals were anesthetized in a Halothane/O_2 atmosphere and dorsal hair was removed. The shaved dorsum of 8 opossums was treated with 100 μl of 0.5% DMBA in ethanol on Monday and Thursday of week 1. At week nine, the average number of melanocytic lesions greater than 1 mm in diameter per animal was 11.8 ± 4.3 (mean ± standard deviation). One or more of these lesions on each animal has progressed over a two-year period to melanomas. Melanomas on three of the animals have metastasized to lymph nodes, liver, spleen and lungs. Seventy-six weeks following DMBA treatment, a total of 26 melanocytic lesions on four of the surviving five animals were analyzed by ESS while animals were anesthetized.

2.3. Histopathology

While the animals were anesthetized, 13 melanocytic lesions were removed for histopathologic examination. The samples were fixed in 10% neutral buffered formalin, embedded in paraffin, sectioned at 5 microns and stained with hematoxylin and eosin. Following microscopic examination, the lesions were classified as melanoma or benign lesions based on lesion depth and cellular morphology.

2.4. Optical Biopsy Systems

The general principles of elastic-scattering spectroscopy (ESS) and the operating features of the optical systems have been described in several earlier publications (5,7). Although not previously described in those publications, the NIR system operates in the same manner as the UV-visible system, but the spectrometer utlizes an InGaAs linear array (Control Develpment, Inc.). Both portable UV-visible and near infrared (NIR) ESS systems use the same fiber-optic probe geometry. The core diameters for illuminating and collecting fibers were 400 and 200 μm, respectively, with center-to-center separation of 350 μm. At this small separation, the collected light is sensitive to both scattering and absorption properties of tissue (3,4). The UV-visible system uses a pulsed broadband Xenon arc lamp as the light source, which covers the spectral range of 330-900 nm. The NIR light source was a continuous broadband incandescent lamp that covers the spectral region of 900-1700 nm. The ESS probe is placed in optical contact with the tissue under investigation. All measurements reported in this paper were taken in the presence of ambient illumination with background subtraction, and calibrated against a spectrally flat-diffuse reflector (Spectralon®). Thus, the spectra were calculated according to the following equation.

$$I(\lambda)=[I(\lambda)_{tissue} - I(\lambda)_{background}]/\ [I(\lambda)_{ref} - I(\lambda)_{background}],$$

where $I(\lambda)_{tissue}$ is the measured spectrum of the tissue site being examined, $I(\lambda)_{background}$ is the ambient and dark-noise taken with the excitation lamp off, and $I(\lambda)_{ref}$ is the diffuse-reflectance reference measured with the flat-diffuse reflector.

The resulting spectra, $I(\lambda)$, were then normalized either to the total area under the whole curve (UV-visible) or to a given spectral point (NIR). In the UV-visible ESS, the area difference between the trapezoid formed at the boundaries of the range of 400-650 nm and the corresponding spectral curve was used to distinguish malignant melanoma from benign lesions. The NIR-ESS spectra were normalized to unity at the wavelength 1340 nm, chosen because there is minimal water absorption at this wavelength. The area under the curve covering the range of 920-1200 nm in the normalized spectra served as the distinction criterion.

3. RESULTS AND DISCUSSION

The 13 biopsied lesions were analyzed by two standard histopathological procedures. The first one is based on lesion depth in the dermis and the cellular morphology. Using this procedure, the samples were classified as following: 5 melanoma, 4 undecided, 3 benign lesion and 1 normal. The second procedure is based solely on cellular morphology in the lesion mass. The results of this procedure disagree somewhat with the previous findings in that 3 of the 4 undecided samples as benign lesions.

The typical spectra measured using the UV-visible ESS System for normal skin, pigmented benign lesions and melanoma are shown in figure 1. These spectra were normalized to have the same total area under the curve, and they are representative of the averages of the three types of examined tissues.

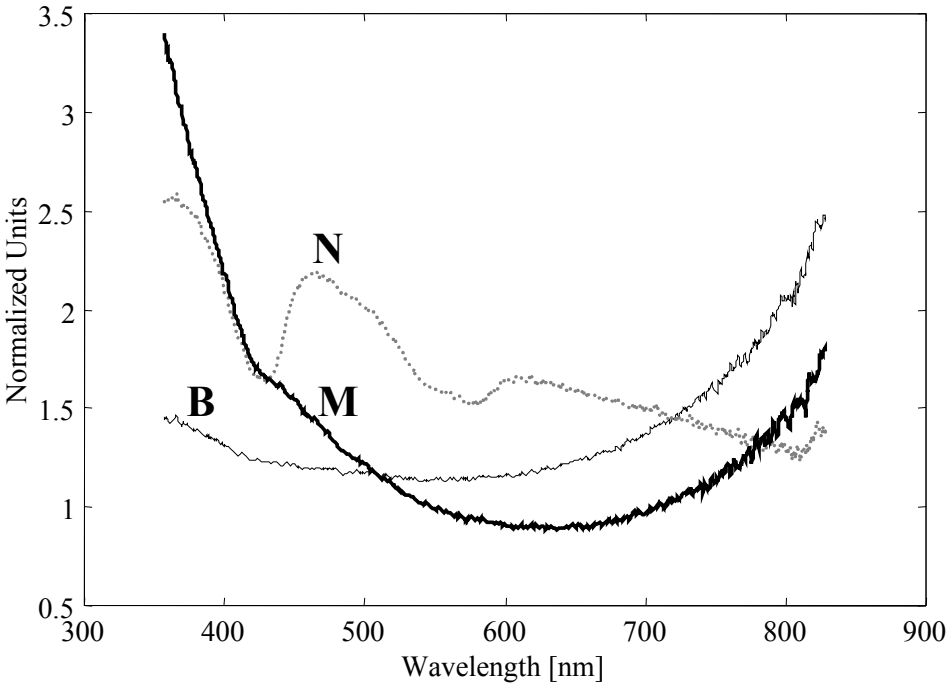

Figure 1. Normalized elastic-scattering spectra representative of typical data for normal skin, pigmented benign lesion and melanoma measured on opossums using UV-visible Optical Biopsy system. N: normal skin, B: benign pigmented lesion and M: melanoma.

The melanin, which strongly absorbs light in the UV-visible region, is the major chromophore in the pigmented lesions (8). If the absorption process due to melanin were dominant, the spectral region from 330 to 600 nm should be strongly attenuated. The spectral shape of melanoma for this range is surprising, in that the scattering appears to be stronger than absorption. It is possible that melanin itself also acts as a strong Rayleigh scatterer (9). This hypothesis is supported by the fact that we were able to observe a very slight absorption effect due to the hemoglobin Soret-band (≈413 nm) in the melanoma lesions, but the absorption effect due to melanin is weak. Taking into account that the probe geometry is sensitive to both scattering and absorption, we observe that the cellular morphology appears to have strong effect on the shape of spectra than the content of chromophores for this kind of highly pigmented melanoma. The normal skin spectrum shows obvoius features due to hemoglobin absorption bands (≈ 413, 540 & 580 nm). The benign-lesion spectrum is relatively featureless except for the strong attenuation in the range of 330-600 nm, due to melanin absorption. Based on the spectral shape for the lesions, we found that the range of 400-650 nm provides the most significant difference between benign lesions and melanoma. The area difference between the trapezoid formed at the boundaries of this range and the corresponding spectral curve was used to distinguish malignant melanoma from benign lesions for UV-visible ESS. The normal skin was not considered for this particular analysis, as the distinctive and reproducible shape of its scatter spectrum was sufficient to provide adequate discrimination, and the interesting problem is to distinguish benign and malignant lesions.

Figure 2 shows a scatter plot of the area difference criterion as a function of the biopsied lesions. Plot (A) is correlated to the findings of the first histopathological procedure, which is based on the lesion depth in the dermis, as well as the cellular morphology. Plot (B) is correlated to the findings of the second procedure, which is based solely on the cellular morphology in the lesion mass. The symbols (+), (∗) and (⊕) represent benign lesions, undecided and malignant melanoma, respectively, according to the histopathology. The UV-visible ESS provided good correlation for 11/13 lesions. Two "misclassified" lesions grouped spectrally with malignant melanomas. However, it is important to underline here that one of them was classified undecided by both of the histopathological procedures. The other one was classified undecided by the first procedure and benign by the second.

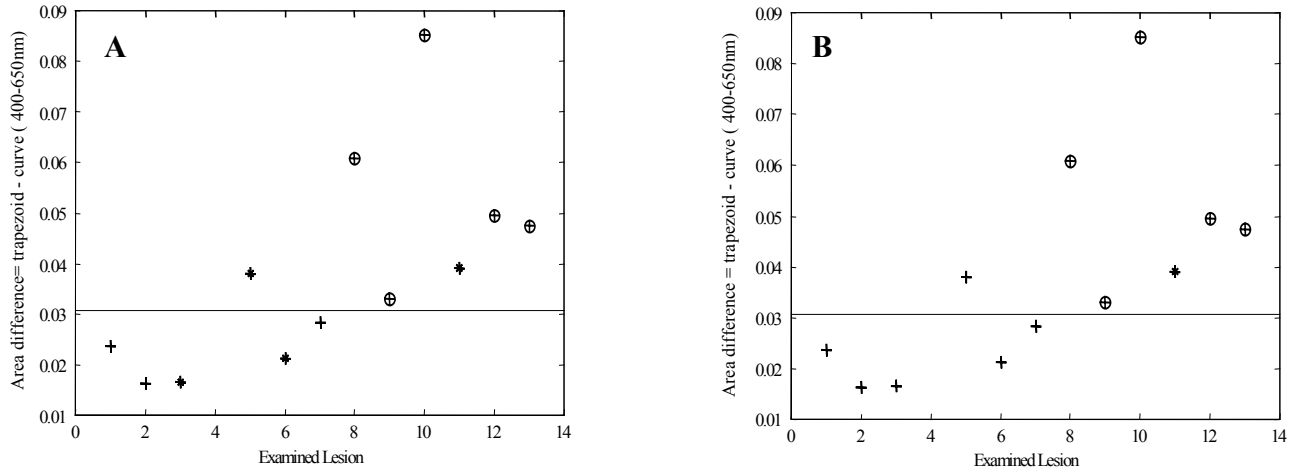

Figure 2. Scatter plot of the area difference between the spectra and the trapezoid formed at the boundaries of the range of 400-650 nm, as a function of the examined lesions. In plot (A) the symbols correlate to the findings of the first histopathological procedure, which is based on the lesion depth in the dermis and the cellular morphology. In plot (B) the symbols correlate to the findings of the second procedure, which is based solely on the cellular morphology in the lesion mass. The symbols (+), (∗) and (⊕) represent benign lesions, undecided and malignant melanoma, respectively.

Figure 3 shows the NIR-ESS scatter spectra for normal skin, pigmented benign lesions and melanomas. The spectra were normalized to unity at the wavelength 1340 nm, chosen because there is minimal water absorption at this wavelength. The spectra are representative of the averages of the three types of examined tissues. The common feature among the three kinds of tissue is the absorption band due to water at around 1450 nm. The full width at half maximum (FWHM) of the melanoma scatter spectrum in the range of 920-1400 nm is significantly larger than that of benign lesions. Moreover, a slight feature around 1150 nm also distinguishes the melanoma scatter spectra from that of benign nevi. The area under the curve covering the range of 920-1200 nm in the normalized spectra was used as the distinction criterion. Again, the normal skin was not included in this analysis. The spectrum for normal skin shows a slight absorption feature due to water, around 1200 nm, which does not appear either in benign lesions or melanoma. Figure 4 shows a scatter plot of the 920-1200 area criterion as a function of the biopsied lesions. As in figure 2, plot (A) is correlated to the findings of the first histopathological procedure, based on the lesion depth in the dermis and the cellular morphology, and plot (B) correlates to the findings of the second procedure, based solely on the cellular morphology in the lesion mass. As before, the symbols (+), (∗) and (⊕) represent benign lesions, undecided and malignant melanoma, respectively. Using the area (920-1200 nm) distinction criterion NIR-ESS showed good correlation for 12/13 lesions. The "misclassified" lesion grouped with the benign lesions spectrally; however, it was classified undecided by both of the histopathological procedures.

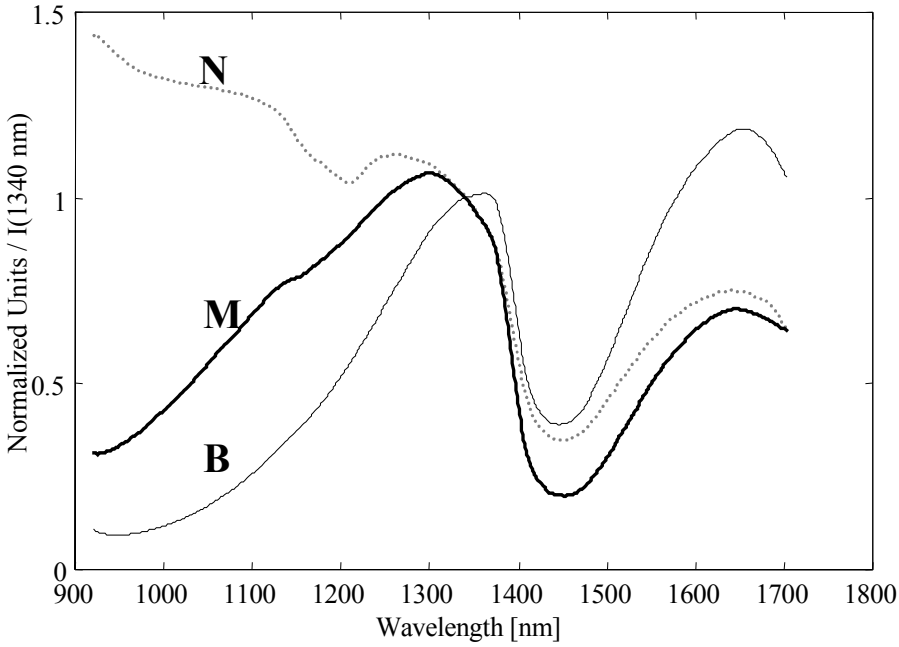

Figure 3. Normalized elastic-scattering spectra representative of typical data for normal skin, pigmented benign lesion and melanoma measured on opossums using NIR Optical Biopsy system. N: normal skin, B: benign pigmented lesion and M: melanoma.

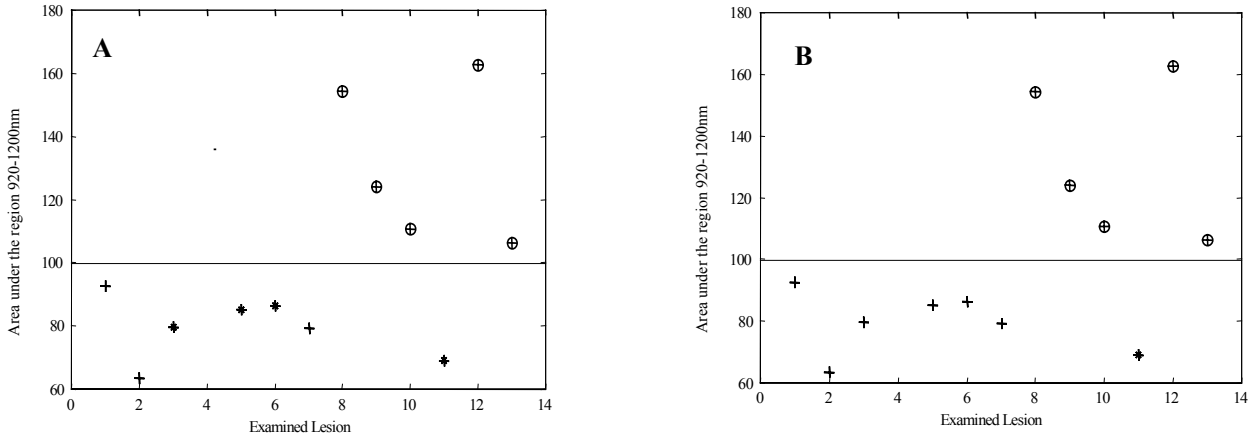

Figure 4. Scatter plot of the area under the curve for the range of 920-1200 nm in the normalized spectra as a function of the examined lesions. In plot (A) the symbols correlate to the findings of the first histopathological procedure, which is based on the lesion depth in the dermis and the cellular morphology. In plot (B) the symbols correlate to the findings of the second procedure, which is based solely on the cellular morphology in the lesion mass. The symbols (+), (∗) and (⊕) represent benign lesions, undecided and malignant melanoma, respectively.

Table 1 summarizes the findings of the histopathological procedures in comparison with the results obtained by ESS. Analysis of these data shows that both UV-visible and NIR elastic-scattering spectroscopy provide spectral criteria that correlate repeatably with the histopathological procedure that is based solely on cellular morphology more than the histopathological procedure that is based on both lesion depth in the dermis and cellular morphology. Both UV-visible and

NIR methods are sensitive to cellular morphology, but do not assess lesion depth. Consequently, it is reasonable that we get consistent correlation with the second histopathological procedure (B), while the first procedure (A) provides more undecided diagnoses, for which no correlation is possible. Nonetheless, ESS did produce consistent correlation with the first procedure (A) for the unambiguous samples.

Animal	Lesion	Lesion depth in the dermis & cellular morphology findings (A)	Cellular morphology findings (B)	UV-visible ESS Findings	NIR-ESS Findings
1	1	Benign	Benign	Benign	Benign
	2	Benign	Benign	Benign	Benign
	3	Undecided	Benign	Benign	Benign
	4	Normal Skin	Normal Skin	Normal Skin	Normal Skin
2	5	Undecided	Benign	Melanoma	Benign
	6	Undecided	Benign	Benign	Benign
	7	Benign	Benign	Benign	Benign
3	8	Melanoma	Melanoma	Melanoma	Melanoma
	9	Melanoma	Melanoma	Melanoma	Melanoma
	10	Melanoma	Melanoma	Melanoma	Melanoma
4	11	Undecided	Undecided	Melanoma	Benign
	12	Melanoma	Melanoma	Melanoma	Melanoma
	13	Melanoma	Melanoma	Melanoma	Melanoma

Table 1: Comparison between the histopathological findings and ESS results.

4. CONCLUSION

ESS is a sensitive technique for detecting changes in cell morphology that accompany the transformation of normal cells to cancerous cells. The results of this experiment showed that both UV-visible and NIR-ESS have the potential to classify the skin lesions with encouraging correlation to diagnosis provided by standard histopathological examination. Ultimate utility cannot be determined from such a small data set, and the relevance of data from this animal model to optical detection of melanoma in human cannot be assumed, but these results do encourage for this study.

5. ACKNOWLEDGEMENTS

The authors would like to thank Dr. D. K. Kusewitt for the histopathology analysis.

REFERENCES

[1] Irving J. Bigio and Judith R. Mourant. "Ultraviolet and visible spectroscopies for tissue diagnostics: fluorescence spectroscopy and elastic-scattering spectroscopy." *Physics in Medicine and Biology,Vol. 42, pp. 803-813, (1997)*.

[2] Irving J. Bigio, Tamara M. Johnson, Judith R. Mourant, Bruce J. tromberg, Yona Tadir, Mathias Fehr, Henrik Nilsson and Vicki C. Darraw. "Determination of the cervical transformation zone using elastic-scattering spectroscopy." *SPIE Proceeding, Advances in Laser and Light Spectroscopy to Diagnose Cancer and Other Diseases III: Optical Biopsy. Vol. 2679, pp. 85-91, 1996*.

[3] Judith R. Mourant, Irving J. Bigio, Darren A. Jack, Tamara M. Johnson, and Heather D. Miller. "Measuring absorption coefficients in small volumes of highly scattering media: source-detector separation for which path lengths do not depend on scattering properties." *Applied Optics, Vol. 36, No. 22, pp. 5655-5661, 1997*.

[4] Judith R. Mourant, Tamika Fuseilier, James Boyer, Tamara M. Johnson, and Irving J. Bigio. "Predictions and measurements of scattering and absorption over broad wavelength ranges in tissue phantoms. *Applied Optics, Vol. 36, No. 4, pp. 949-957, 1997*.

[5] Judith R. Mourant, Irving J. Bigio, James Boyer, Tamara M. Johnson, JoAnne Lacey, Antony G. Bohorfoush, and Mark Mellow. "Elastic-scattering spectroscopy as a diagnostic tool for differentiating pathologies in the gastrointestinal tract: preliminary testing.", *Journal of Biomedical Optics, Vol. 1(2), pp.192-199, 1996.*

[6] Judith R. Mourant, Andreas H. Hielscher, Angelia A. Eick, Dan Shen, Tamara M. Johnson, James P. Freyer. "Evidence of intrinsic differences in the light scattering properties of tumorigenic and nontumorigenic cells." *Cancer (Cancer Cytopathology), Vol. 84, No. 6, pp. 366-374, 1998*.

[7] Judith R. Mourant, Irving J. Bigio, James Boyer, Richard L. Conn, Tamara M. Johnson, and Tsutomu Shima. "Spectroscopic diagnosis of bladder cancer with elastic light scattering." *Lasers in Surgery and Medicine, Vol. 17, pp. 350-357, 1995.*

[8] V. P. Wallace, D. C. Crawford, P. S. Mortimer, R. J. Ott and J. C. Bamber. "Specrophotometric assessment of pigmented skin lesions: methods and feature selection for evaluation of diagnostic performance." *Physics in Medicine and Biology, Vol. 45, pp. 735-751, 2000.*

[9] M. L. Wolbarsht, A. W. Walsh and G. George,. " Melanin, a unique biological absorber." *Applied Optics, Vol. 20, pp. 2184-6, 1981.*